International Journal of Control and Automation
Vol. 7, No. 12 (2014), pp. 155-164
http://dx.doi.org/10.14257/ijca.2014.7.12.15

A Parameter Selection Model for Avascular Tumor Growth

Changyu Liu [1, 4], Bin Lu [2, *], Cong Li [3]

[1]*School of Computer Science and Engineering, South China University of Technology, Guangzhou 510006, China*
[2]*School of Computer Science, Wuyi University, Jiangmen 529020, China*
[3]*College of Computer Science, Sichuan Normal University, Chengdu 610068, China*
[4]*School of Computer Science, Carnegie Mellon University, Pittsburgh, PA 15213, USA*
*yezhich@gmail.com, *lbscut@gmail.com (corresponding author), jkxy_lc@sicnu.edu.cn*

Abstract

Based on a set of reaction-diffusion equations of oxygen, glucose and growth inhibitory factor which were built to describe the tumor growth environment, a cell cycle control factor was proposed for the simulation of the avascular tumor growth. In order to fix the model parameters, a two-level heuristic searching was given for the parameter selection. Finally, a total finite element energy equation was present to combine the chemical simulation and the physical simulation for the avascular tumor growth. Experimental results showed that the presented approach outperformed the baseline approach in the simulation of the mouse mammary tumor cells EMT6/Ro.

Keywords: *parameter selection, avascular tumor growth, reaction-diffusion equations*

1. Introduction

The difficult issues for tumor prevention and cure lie in a lack of understanding for the internal process and mechanism of tumor growth. Hence, the mathematical modeling for the fundamental mechanism of tumor growth becomes a hot research topic in fields of theoretical biology and mathematics. The Cellular Potts Model (CPM) [1] is a simple but flexible framework for cell-oriented models of development. It has been used for modeling many morphogenesis processes, including cell sorting [2], tumor growth [3], vascularization [4-5], angiogenesis [6], limb growth [4] and slime mold development [7]. Specifically, Jiang *et al.* [3] proposed a multi-scale avascular tumor growth model, which includes a cell cycle, a protein regulatory network and extra cellular chemical dynamics, to study the avascular growth of the EMT6/Ro mouse mammary tumor [8]. Kejing He *et al.* [9] proposed a hybrid parallel framework for the Cellular Potts Model simulations to solve the time-consuming partial differential equation (PDE), cell division and cell reaction operation of a large scale simulation ($\sim 10^6$) by using the Message Passing Interface (MPI).

Due to the fact that the tumor growth is a complex process that involves a cell cycle, a cell interaction and an extracellular microenvironment, the traditional cellular Potts model (CPM) and some other extensions of it [10] are not only too simple to simulate the dynamic microcosmic process of the tumor growth, but also too simple to model the internal principles of chemical diffusion and chemical restriction for the tumor growth. In this paper, a two-level parameter selection and a cell cycle control factor were proposed for the simulation of the avascular tumor growth based on the existing CPM [11]. The proposed approach considered a cell cycle control factor, a cell dynamic process, a cell

ISSN: 2005-4297 IJCA

interaction, a chemical environment, and a finite element approach for solving two kinds of key differential equations, which are a set of reaction-diffusion equations for describing the chemical microenvironment, such as nutrients (oxygen and glucose), metabolic waste, growth promoters and inhibitors [3], and a set of finite element equations that contains a total energy expression of cell surface adhesion and cell space competition.

2. Reaction Diffusion Equation

Reaction diffusion equation plays an important role for a simulation of the avascular tumor growth. In this paper, we assume that there are three layers, which are a proliferating (P) layer, a quiescent (Q) layer and a necrotic (N) layer from outside to inside in a growth saturated avascular tumor spheroid, and that there is a competition for nutrients among the tumor cells, while there is no such competition between the normal cells and the tumor cells. There are mainly two kinds of chemical substances that influenced the tumor growth in its extracellular microenvironment. One of them is the nutrient which refers to oxygen and glucose. The other is the Growth Inhibitory Factor (GIF), such as vascular endothelial growth factor (VEGF), vascular permeability factor (VPF), transforming growth factor TGF beta 1and TGF beta 2. Such influences are expressed by its local concentrations through a set of reaction-diffusion equations. This paper proposed a new set of reaction diffusion equations, as shown in Eq. (1) and Eq. (2), based on paper [12].

$$\frac{\partial N(\vec{x},t)}{\partial t} = \overrightarrow{D_N}\nabla^2 N(\vec{x},t) - \sigma\overrightarrow{\alpha_N}\overrightarrow{K_N}N(\vec{x},t) \tag{1}$$

$$\frac{\partial G(\vec{x},t)}{\partial t} = D_{GIF}\nabla^2 G(\vec{x},t) - \sigma\alpha_{GIF}K_{GIF}G(\vec{x},t) + \sigma[G_M - G(\vec{x},t)]\vec{\Gamma}N(\vec{x},t) \tag{2}$$

where $\vec{x} = (x,y,z)^T$ is a three dimension coordinates vector, $N(\vec{x},t) = (N_O, N_G)^T$ is a concentration field vector of oxygen and glucose, $\overrightarrow{D_N} = diag(D_O, D_G)$ is the diffusion constants diagonal matrix, $\overrightarrow{\alpha_N} = diag(\alpha_O, \alpha_G)$ is the control constants diagonal matrix, σ is the tumor cell number, $\overrightarrow{K_N} = diag(K_O, K_G)$ is the consumption rates diagonal matrix with $K_O \in \{K_O^P, K_O^Q, K_O^N\}$ and $K_G \in \{K_G^P, K_G^Q, K_G^N\}$, $G(\vec{x},t)$ is the GIF concentration field, D_{GIF} is the GIF diffusion constants, α_{GIF} is the GIF control constants diagonal matrix, $K_{GIF} \in \{K_{GIF}^P, K_{GIF}^Q, K_{GIF}^N\}$ is the GIF degradation rate, $\vec{\Gamma} = (\Gamma_O, \Gamma_G)$ is the GIF saturation rate vector, $G_M = G_{GIF}^{THR}$ is the saturation value. As shown in Algorithm 1, we construct a Partial Differential Equations (PDE) solver for our reaction diffusion equation.

Algorithm 1: FEM based reaction diffusion equation solver

Input:

Initial Concentrations: N_O^{INT}, N_G^{INT}, G_{GIF}^{INT};
Concentrations Threshold: N_O^{THR}, N_G^{THR}, G_{GIF}^{THR};
Constant coefficients: $\overrightarrow{D_N}$, D_{GIF}, σ, $\overrightarrow{\alpha_N}$, α_{GIF}, $\overrightarrow{K_N}$, K_{GIF}, G_M, $\vec{\Gamma}$.

Output:

$N(\vec{x},t)$ and $G(\vec{x},t)$.

1: Initialize FEM mesh with using a circle PDE geometry;
2: Refine twice this mesh with the same geometry;
3: Get Point matrix *p*, Edge matrix *e* and Triangle matrix *t*;
4: Set concentration with: $N(\vec{x},0) \leftarrow [N_O^{INT}, N_G^{INT}]$; $G(\vec{x},0) \leftarrow G_{GIF}^{INT}$;
5: Set the PDE boundary Ω, with
6: $\quad \vec{h}\vec{u} = \vec{r}$;

7: $\vec{n} \cdot (\vec{c} \otimes \nabla \vec{u}) + q\vec{u} = \vec{g} + \vec{h}'\mu$;
8: Set: $d \leftarrow [1;1]$; $c \leftarrow [\overrightarrow{D_N}]$; $a \leftarrow [\sigma\overrightarrow{\alpha_N}\overrightarrow{K_N}]$; $f \leftarrow [0;0]$;
9: Get $N(\vec{x},t)$ by solving parabolic PDE: $d(\partial u/\partial t) - \nabla \cdot (c\nabla u) + au = f$ on Ω;
10: Set: $d \leftarrow 1$; $c \leftarrow D_{GIF}$; $a \leftarrow \sigma\alpha_{GIF}K_{GIF} + \sigma\vec{\Gamma}N(\vec{x},t)$; $f \leftarrow \sigma G_M\vec{\Gamma}N(\vec{x},t)$;
11: Get $G(\vec{x},t)$ by solving parabolic PDE: $d(\partial u/\partial t) - \nabla \cdot (c\nabla u) + au = f$ on Ω;
12: Return $N(\vec{x},t)$ and $G(\vec{x},t)$.

3. Cell Cycle Control Factor

During a cell cycle, there are one resting phase G_0 for quiescent cells and four growth phases [13], which are: (1) First Growth Phrase (G_1). During G_1 phase, the cell grows in size and synthesizes mRNA and proteins, such as cyclins, CDKs (cyclin-dependent kinases), CKIs (cycline kinase inhibitors), and the anaphase-promoting complex, that are required for DNA synthesis. If the required proteins and growth are unaccomplished, the cell enters G_0 phase, otherwise it would enter the next *S* phase of the cell cycle, which was also called a G_1-*S* phase transition. (2) Synthesis Phase (*S*). This phase is mainly for DNA replication and chromosomes replication. (3) Second Growth Phase (G_2). This phase is for a preparation of the mitosis growth. (4) Mitotic Phase (*M*). This phase consists of a prophase, a metaphase, an anaphase and a telophase.

Since the key role that played by the G_1-*S* phase transition, we assumed that there are three growth results after this progress: (1) Toward a cell division (also proliferating or mitosis) status if the cell met the G_1-*S* transition condition and it hasn't been divided before. (2) Toward a cell quiescent status if the cell didn't meet the G_1-*S* transition condition and it hasn't been divided before. (3) Otherwise toward a cell necrotic or shedding status. Based on these assumptions, this paper proposed a cell cycle control factor that played a same role as a proteins list [3] of GSK3b, TGFb, SMAD3, SMAD4, SCF, CDK inhibitors 4a–d, Kip 1, 2 (p27, p57), Cip1 (p21), cyclinsD and E, Rb, and E2F in the whole tumor cell cycles.

$$F(\vec{x},t) = 1 - exp\{\frac{\vec{\delta}[N(\vec{x},t) - N^{THR}]}{\theta[2 - exp(-\sigma/\sigma_0)][G(\vec{x},t) - G_{GIF}^{THR}]}\} \tag{3}$$

where $F(\vec{x},t)$ is a cell cycle control factor of a specific tumor cell, $\vec{\delta} = (\delta_O, \delta_G)$ is a constant vector for deciding the influence of oxygen and glucose on the local GIF factor level, $N(\vec{x},t)$ is the concentration field vector of nutrients, $N^{THR} = (N_O^{THR}, N_G^{THR})^T$ is the concentration threshold vector of the nutrients, below which the tumor cells' reproduction is inhibited, σ is the number of tumor cells, σ_0 is a influence constant of cell number on the cell cycle control factor, θ is a shape parameter for sigmoid function, $G(\vec{x},t)$ is the concentration field of GIF, G_{GIF}^{THR} is the threshold of the GIF.

There are some benefits with using our cell cycle control factor: (1) the $F(\vec{x},t)$ plays a key role in our model. we define: if $F(\vec{x},t) \leq 0$ the cell will become necrotic, if $0 < F(\vec{x},t) \leq F^{THR}$ the cell will become quiescent, and if $F^{THR} \leq F(\vec{x},t) \leq 1$ the cell will become proliferating. (2) nutrients concentration field $N(\vec{x},t)$ was introduced to reflect that the cell cycle could be controlled by its surrounding nutrients concentration field and the neighbor cells could have a competition with each other for such nutrients. (3) tumor cells number σ was also applied to denote this competition. (4) GIF concentration field $G(\vec{x},t)$ was also adopted to simulate the influence of a list of proteins on the intracellular cycle. (5) our cell cycle control factor could integrate well with the finite element based tumor growth modeling with a set of total energy equations.

4. Parameter Selection

We also assume that: (1) the distribution range of $F(\vec{x},t)$ should fill the whole [0, 1] as much as possible. We consider

$$L(\theta) = F(\vec{x},t_0,\theta) - F(\vec{x},t_n,\theta) \tag{4}$$

where t_0 is the starting time and t_n is the finishing time for tumor growth simulation. We then select θ that makes $L(\theta)$ as near to 1 as possible. (2) the mean value of $F(\vec{x},t)$ should be near 0.5. So, we consider arithmetic mean index

$$E(\theta) = \sum_{t=t_0}^{t_n} \frac{F(\vec{x},t,\theta)}{t_n - t_0} \tag{5}$$

and let $F^{THR} = E(\theta)$, $|E(\theta) - 0.5| \leq \Delta$, where $\Delta = 0.2$ is a control parameter. In order to use parameter selection method to analyze the relation between parameter θ and cell cycle control factor $F(\vec{x},t)$, we firstly set the initial chemicals (oxygen, glucose, GIF) concentration to be (0.08 mM, 5.5mM, 0 mM), and then took the average chemical concentration in the tumor spheroid as an input of $N(\vec{x},t)$ or $G(\vec{x},t)$, where $\vec{x}$ is sampled in the center point between the spheroid center and its surface at the step time 0:30:300 after the solving of chemical reaction diffusion equation. The numerical concentrations of chemicals on sampled steps are shown in Table 1.

Table 1. Numerical Concentrations of Chemicals on Sampled Steps

Steps	0	30	60	90	120	150	180	210	240	270	300
Oxygen	0.0800	0.0712	0.0557	0.0458	0.0436	0.0427	0.0418	0.0392	0.0385	0.0376	0.0365
Glucose	5.5000	4.7183	3.5452	2.7632	2.6298	2.5452	2.4571	2.3673	2.2792	2.1833	2.0973
GIF	0.0000	1.1534	2.5451	7.1308	12.5666	14.6314	15.7945	17.9261	19.0378	19.8484	20.5136

Due to the θ is determined implicitly by $F(\vec{x},t)$ with a specific initial chemical concentrations, a heuristic searching approach for the most suitable parameter θ in a value space was introduced in this paper. Through many experiments with a wide range of initial chemical concentrations, the ranges of θ are all within (0, 5]. A multi-scale space searching method was applied for saving search time. We set θ to be 1:1:5 in the loose search and search the one that makes $L(\theta)$ as big as possible, as shown in Figure 1a and Figure 1b. It can be seen that: (1) the value of $F(\vec{x},t)$ decreased with the simulation time for a specific θ. (2) the value of $F(\vec{x},t)$ increased with the growing of parameter θ for a specific simulation time. (3) In all these case, a $\theta = 1$ make the value of $L(\theta)$ at a maximum. So, the loose searching result is $\theta = 1$.

Since we get $\theta = 1$ in the loose search, we can then proceed to conduct a fine search for the optimum θ in $(\theta - 0.9):0.1:\theta$. Firstly, compute and sort $L(\theta)$ for each θ in $(\theta - 0.9):0.1:\theta$ from big value to small value. Secondly, delete the θ that makes $|E(\theta) - 0.5| > \Delta$ from the sorted sequence. Finally, take the first value θ of the sorted sequence for the optimum solution of our model. The distribution of $F(\vec{x},t)$ in the fine search shows a same trend as that of loose search, as shown in the Figure 1c and Figure 1d. It can be seen that: (1) the value of $F(\vec{x},t)$ fills more area of [0, 1] for the fine search. (2) the value of $L(\theta)$ reaches a maximum and $|E(\theta) - 0.5| \leq \Delta$ when θ equals to 0.3 for the initial concentrations. Thus, the final fine search result is: $\theta = 0.3$ and $F^{THR} = 0.4381$ for the initial concentrations at (0.08 mM, 5.5mM, 0 mM). Once got the value of θ through parameter search, we can then proceeded to simulate the whole tumor growth.

5. Growth Simulation

According to Jiang *et al.* 's [3] multi-scale avascular tumor growth model, the total energy (Hamiltonian function, H) is a kind of cell interactions through surface adhesion and space competition after partitioned by a discrete lattice Monte Carlo model on the three-dimensional space into domains of cells and cell medium, and can be defined as

$$H = \sum_{lattice\ sites} J_{\tau(S_1)\tau(S_2)}[1 - \delta(S_1, S_2)] + \sum_{cells} \gamma(V - V^*)^2 \quad (6)$$

where H is an effective total energy, S_1 and S_2 denote two tumor cell entities which occupy two discrete lattice coordinates $S_1(x, y)$ and $S_2(x, y)$, $J_{\tau(S_1)\tau(S_2)}$ corresponds to the adhesive energy between cell S_1 and cell S_2, $\delta(S_1, S_2)$ is the Kroneker function which was defined as: if $i = j$, it value will be 1, otherwise will be 0, V is the current cell volume while V^* is the target cell volume, which normally is twice the volume of a new cell, and γ is the coefficient corresponding to the elasticity of the cell volume. It can be seen from this total energy equation that the cell growth with an increase of its volume and surface area will consume the total energy.

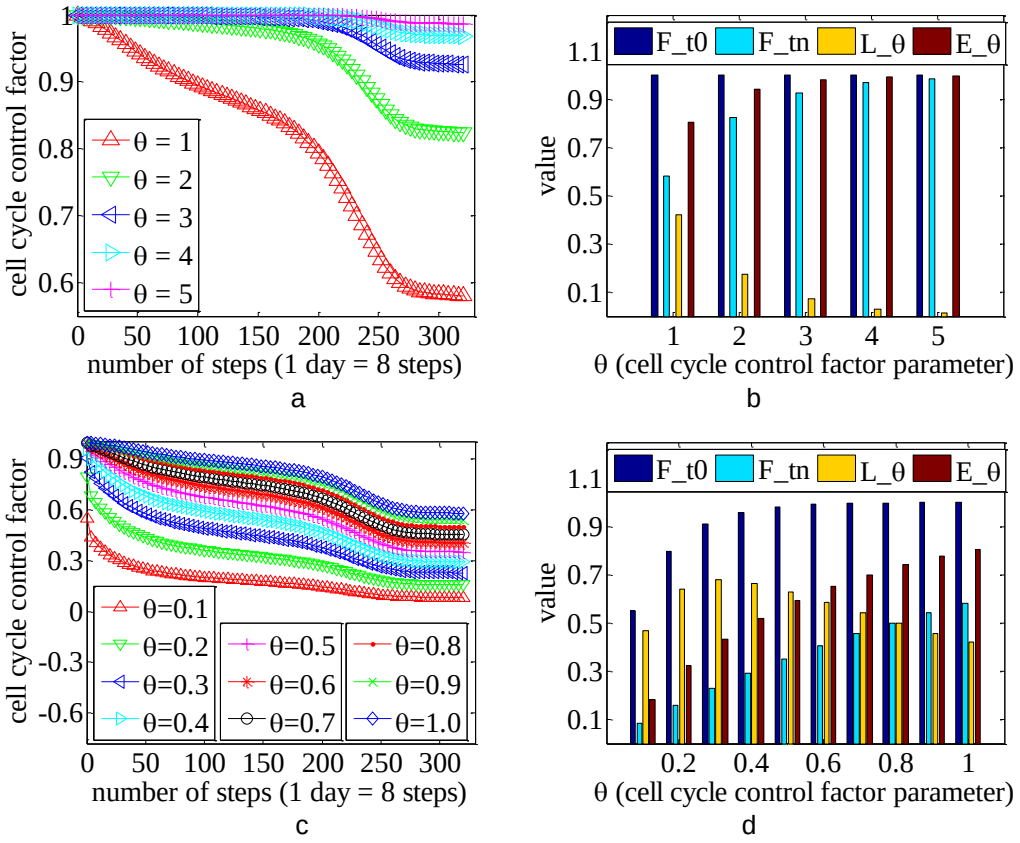

Figure 1. Parameter Selection for θ and F^{THR}. (a-c) the Relation between Cell Cycle Control Factor and θ for the Loose Search and the Fine Search Respectively, (b-d) the Histograms of $F(t_0)$, $F(t_n)$, $L(\theta)$ and $E(\theta)$ for the Loose Search and the Fine Search Respectively

In order to consider an extracellular microenvironment, an intracellular cycle and a finite element approach, this paper introduced the proposed cell cycle control factor into

the total energy Eq. (6) to form our finite element (FEM) tumor growth model, as shown in Eq. (7).

$$H = \sum_{A=1}^{AN} J_A S_A + \sum_{C=1}^{CN} \gamma (V_C - V_C^*)^2 \qquad \text{and} \qquad V_C^* = [1 + \lambda F(\vec{x}, t)] V_C \tag{7}$$

where AN is the global total mesh surface number, CN is the total cell number, A is the global mesh surface identifier that among 1~ AN, C is the cell identifier that among 1~ CN, S_A is the current area of mesh surface A, V_C is the current volume of cell C while V_C^* is its target cell volume, $J_A \in \{J_A^{PP}, J_A^{PQ}, J_A^{PN}, J_A^{QQ}, J_A^{QN}, J_A^{NN}\}$ is the adhesive coefficient between mesh surface A and its neighbours, $\gamma \in \{\gamma^P, \gamma^Q, \gamma^N\}$ is the coefficient corresponding to the elasticity of the cell volume of C, $F(\vec{x}, t)$ is a cell cycle control factor and λ is a constant volume amplification factor. In this model, the total energy change H of a tumor cell was determined by its surface, volume and local factor level $F(\vec{x}, t)$.

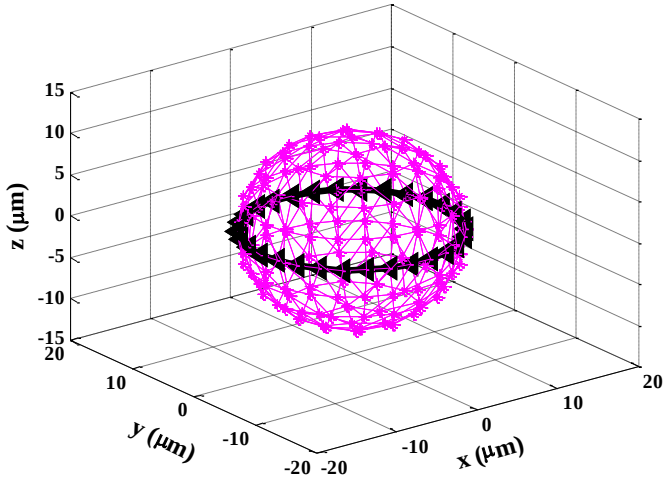

a

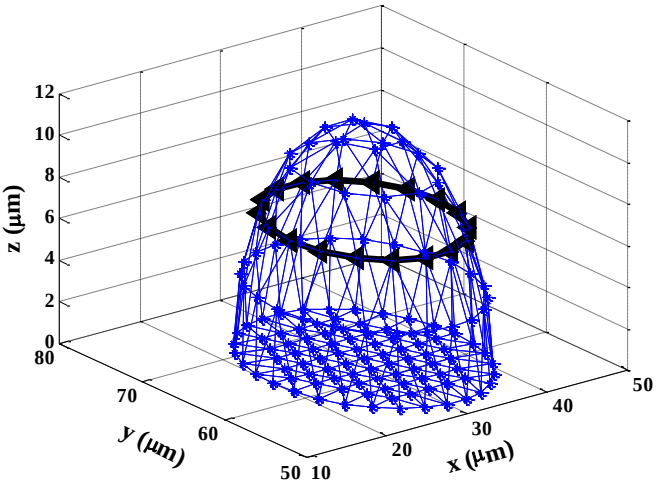

b

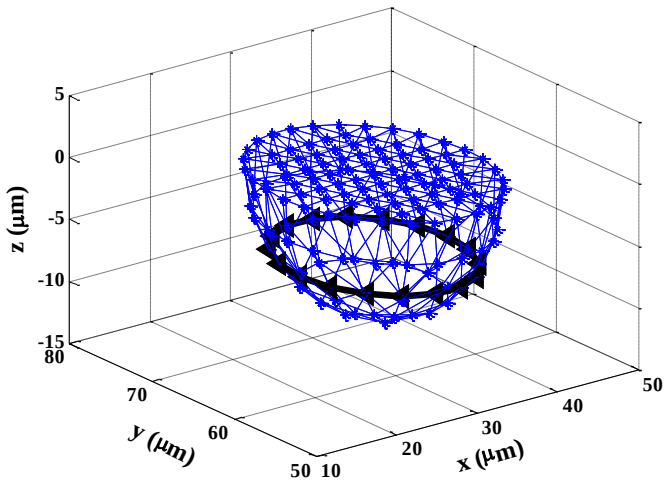

c

Figure 2. Physical Tumor Growth Results. (a) the Initial Tumor Cell at the Origin, (b-c) Two Daughter Cells of the Initial Tumor Cell after a Cell Division

Containing a morphology modeling of the tumor cell surface as well as volume and a chemical modeling of the extracellular microenvironment, the intracellular cycle as well as the cellular tumor growth, our FEM model can simulate well a complex avascular tumor growth. Then, the change of energy ΔH can be uniquely determined by the nodal displacement $\{u\}$. One tumor cell will reach a critical point for division if there is a reasonable displacement $\{u\}$ that leads to minimum ΔH, as

$$\frac{\partial(\Delta H)}{\partial(\{u\})} = 0 \tag{8}$$

It can be seen from Eq. (8) that the tumor growth toward a cell division lies in the solving of the nodal displacement $\{u\}$. In order to get ΔH from Eq. (8), we should know how to model the physic avacular tumor growth by using the Finite Element method. Hence, we constructed an initial cell sphere at the origin. All the physical growths are simulated under parameters: *radius* = 11.2725 μm, *node_number* = 152, *mesh_number* = 300, *center* = origin, and *status* = P. Then, we introduce these initial data to simulate the physical tumor growth under the pre-specified chemical concentrations.

Figure 2 showed some the physic growth results under initial chemicals (oxygen, glucose, GIF) concentrations of (0.08 mM, 5.5mM, 0 mM). We used the black arrows to indicate the cell division boundaries. At the beginning, the cell control factor is larger due to a higher nutrient concentration and a lower growth inhibitor factor concentration. These lead to a rapid tumor spheroid growth if it meets other conditions, such as at a P status or a Q status, and don't reach the target volume.

For mixture tumor growth, the parameters of the mouse mammary tumor cells EMT6/Ro were used, which were derived from our research partner, the Applied Mathematics and Plasma Physics (T-7) group at Los Alamos National Laboratory. We set $\sigma = 1$, $\sigma_0 = 10\text{^}4$, $\vec{\Gamma} = (\Gamma_O, \Gamma_G) = (1,1)$, $\overrightarrow{\alpha_N} = diag(\alpha_O, \alpha_G) = (9 * 10^{-6}, 2 * 10^{-8})$, $\alpha_{GIF} = 8 * 10^{-11}$, $\vec{\delta} = (\delta_O, \delta_G) = (49/50, 1/50)$. We use almost the same setting: $J_A^{PP} = J_A^{PQ} = 28$, $J_A^{PN} = 24$, $J_A^{QQ} = J_A^{QN} = 22$, $J_A^{NN} = 0$ for J_A, and $\gamma^P = 1$, $\gamma^Q = 4$, $\gamma^N = 0$ for γ, as in [3]. Then, we compare our simulation results with Yijiang's

simulation results [3], and with the actual data we obtained from our partner T-7 group based on two indexes, which are the cell number and the cell volume. To keep growth balance, a cell shedding rate of 20% was also applied on cells at the surface of tumor spheroid after its radius exceeds a certain value.

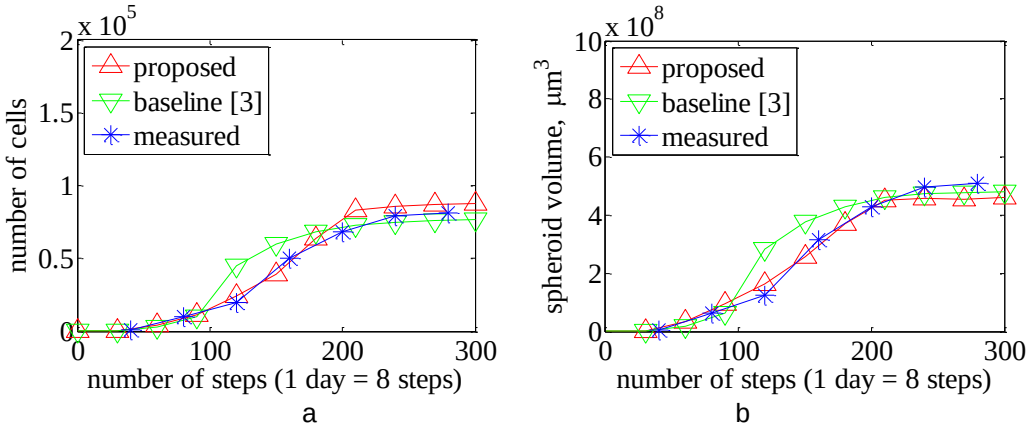

Figure 3. Experiment Results. (a-b) the Total Cell Number and the Total Cell Volume as Functions of Simulation Steps among our FEM Model, the Baseline Model and the Measured Data Separately

According to our experiments, the tumor growth reaches an earlier number saturation state at 30 days or 240 steps, when the division rate equals the shedding rate. With a rapid decrease of proliferating cells, the tumor growth enteres a later saturation state at 40 days or 320 setps. The earlier quiescent cells were generated from cells that don't meet the volume check in the cell cycle. When the chemicals concentration drops below the threshold, those cells may become necrotic. We assume that the GIF was generated by a list of internal control proteins, so the initial concentration of GIF in our simulation is zero. The experiment results were shown in Figure 3. It can be seen that the result from the proposed approach is more close to the measured data than that from the baseline approach. Thus, the proposed approach outperformed the baseline approach.

6. Conclusion

In this paper, we proposed a cell cycle control factor and a two-level parameter selection approach for the simulation of avascular tumor growth. Two sets of equations, which are a set of reaction diffusion equations and a set of total energy equation, were described. Experiments showed that our approach achieved a better agreement with the experimental data from EMT6/Ro mouse mammary tumor spheroids than that from the baseline approach. Further research work will be focused on extending this model to include two following phases, which are an angiogenesis phase and a vascular tumor growth phase.

Acknowledgments

This paper was supported by the Doctor Startup Foundation of Wuyi University under Grant No. 2014BS07, the Basic Theory and Scientific Research Project of Jiangmen City under title "Research on complex network evolution model and link prediction", and the National Natural Science Foundation of China under Grant No. 71202165. We would like to thank anonymous reviewers for helpful comments.

References

[1]. J. Glazier, and F. Graner, "Simulation of the differential adhesion driven rearrangement of biological cells," Phys. Rev. E., vol. 47, no. 3, **(1993)**, pp. 2128-2154.
[2]. R. Chaturvedi, et al., "On multiscale approaches to three-dimensional modelling of morphogenesis," J. R. Soc. Interface., vol. 2, no. 3, **(2005)**, pp. 237-253.
[3]. Y. Jiang, et al., "A multiscale model for avascular tumor growth," Biophys. J., vol. 89, no. 6, **(2005)**, pp. 3884-3894.
[4]. Y. X. Yan, et al., "A downstream mediator in the growth repression limb of the jasmonate pathway," Plant Cell., vol. 19, no. 8, **(2007)**, pp. 2470-2483.
[5]. D. Lyden, et al., "Id1 and Id3 are required for neurogenesis, angiogenesis and vascularization of tumour xenografts," Nature, vol. 401, no. 6754, **(1999)**, pp. 670-677.
[6]. A. L. Bauer, T. L. Jackson, and Y. Jiang, "A cell based model exhibiting branching and anastomosis during tumor-induced angiogenesis," Biophys. J., vol. 92, no. 9, **(2007)**, pp. 3105-3121.
[7]. F. Kuzdzal, et al., "Exploiting new terrain: an advantage to sociality in the slime mold Dictyostelium discoideum," Behav. Ecol., vol. 18, no. 2, **(2007)**, pp. 433-437.
[8]. M. Marusic, Z. Bajzer, J. P. Freyer, and S. V. Pavlovic, "Analysis of growth of multicellular tumor spheroids by mathematical models," Cell Proliferat., vol. 27, **(1994)**, pp. 73-94.
[9]. K. J. He, Y. Jiang, and S. B. Dong, "A hybrid parallel framework for the cellular Potts model simulations," In ICPADS, **(2009)**, pp. 624-631.
[10]. B. M. Rubenstein and L. J. Kaufman, "The role of extracellular matrix in glioma invasion: a cellular Potts model approach," Biophys. J., vol. 95, no. 12, **(2008)**, pp. 5661-5680.
[11]. M. Scianna and L. Preziosi, "Multiscale developments of the cellular Potts model," Multiscale Model. Sim., vol. 10, no. 2, **(2012)**, pp. 342-382.
[12]. S. C. Ferreira, et al., "Reaction-diffusion model for the growth of avascular tumor," Phys. Rev. E, vol. 65, no. 2, **(2002)**, 1907-1–1907-8.
[13]. G. M. Cooper, "The cell: a molecular approach (2nd edition)," ASM Press, Washington, D.C., **(2000)**.
[14]. C. Liu, et al., "A TPSAC model and its application to mechanical cloud simulation," Int. J. Secur. Appl., vol. 8, no. 1, **(2014)**, pp. 45-56.
[15]. J. Folkman, "Tumor angiogenesis factor," Cancer Res., vol. 34, **(1974)**, pp. 2109-2113.
[16]. H. Wang, et al., "Study on behavior simulation for picking manipulator in virtual environment based on binocular stereo vision," In ICSC, **(2008)**, pp. 27-31.
[17]. M. A. J. Chaplain, "Avascular growth, angiogenesis and vascular growth in solid tumours: the mathematical modelling of the stages of tumour development," Math. Comput. Model., vol. 23, no. 6, **(1996)**, pp. 47-87.
[18]. H. Li, et al., "Catalytic hydrothermal pretreatment of corncob into xylose and furfural via solid acid catalyst," Bioresource Technol., vol. 158, **(2014)**, pp. 313-320.
[19]. J. P. Freyer and R. M. Sutherland, "Regulation of growth saturation and development of necrosis in EMT6/Ro multicellular spheroids by the glucose and oxygen supply," Cancer Res., vol. 46, **(1986)**, pp. 3504-3512.
[20]. J. Holash, et al., "Vessel cooption, regression, and growth in tumors mediated by angiopoietins and VEGF," Science, vol. 284, no. 5422, **(1999)**, pp. 1994-1998.
[21]. J. X. Chen, et al., "Modeling and performance analyzing of helix transmission base on Modelica," Key Eng. Mater., vol. 455, **(2011)**, pp. 511-515.
[22]. J. Folkman and M. Hochberg, "Self-regulation of growth in three dimensions," J Exp. Med., vol. 138, no. 4, **(1973)**, pp. 745-753.
[23]. C. Y. Liu, et al., "Research on service-oriented and HLA-based simulation model of juice production line," In ICMTMA, vol. 3, **(2010)**, pp. 167-170.
[24]. H. Greenspan, "Model for the growth of solid tumors by diffusion," Stud. Appl. Math., vol. 51, **(1972)**, pp. 317-340.
[25]. Y. Zhang, Z. He, Y. Zhang, and X. Wu, "Global optimization of wavelet-domain hidden Markov tree for image segmentation," Pattern Recogn., vol. 44, no. 12, **(2011)**, pp. 2811-2818.
[26]. H. L. Li, et al., "One-step heterogeneous catalytic process for the dehydration of xylan into furfural," BioResources, vol. 8, no. 3, **(2013)**, pp. 3200-3211.
[27]. J. A. Adam, "Simplified mathematical model of tumor growth," Math. Biosci., vol. 81, **(1986)**, pp. 224-229.
[28]. S. H. Xu, "Analysis of tumor growth under direct effect of inhibitors with time delays in proliferation," Nonlinear Anal. Real., vol. 11, no. 1, **(2010)**, pp. 401-406.
[29]. H. J. Wang, et al., "Structure design and multi-domain modeling for a picking banana manipulator," Adv. Mater. Res., vol. 97-101, **(2010)**, pp. 3560-3564.
[30]. H. Zhou, Y. H. Yang, N. O. Binmadi, P. Proia, and J. R. Basile, "The hypoxia-inducible factor-responsive proteins semaphorin 4D and vascular endothelial growth factor promote tumor growth and angiogenesis in oral squamous cell carcinoma," Exp. Cell Res., vol. 318, no. 14, **(2012)**, pp. 1685-1698.
[31]. H. Li, et al., "A modified biphasic system for the dehydration of D-xylose into furfural using $SO_4^{2-}/TiO^{2-}ZrO_2/La^{3+}$ as a solid catalyst," Catalysis Today, vol. 234, **(2014)**, pp. 251-256.

[32]. S. H. Xu, M. Bai, and X. Q. Zhao, "Analysis of a solid avascular tumor growth model with time delays in proliferation process," J. Math. Anal. Appl., vol. 391, no. 1, **(2012)**, pp. 38-47.
[33]. C. Liu, et al., "Modeling physical and chemical growths of avascular tumor," Int. J. Multimed. Ubiq. Eng., vol. 9, no. 4, **(2014)**, pp. 349-362.
[34]. T. Roose, S. J. Chapman, and P. K. Maini, "Mathematical models of avascular tumor growth," SIAM Rev., vol. 49, no. 2, **(2007)**, pp. 179-208.
[35]. B. Lu, et al., "Discovery of community structure in complex networks based on resistance distance and center nodes," J. Comput. Inf. Syst., vol. 8, no. 23, **(2012)**, pp. 9807-9814.
[36]. H. Byrne and M. Chaplain, "Free boundary value problems associated with the growth and development of multicellular spheroids," European J. Appl. Math., vol. 8, **(1997)**, pp. 639-658.
[37]. H. Wang, et al., "Study on a location method for bio-objects in virtual environment based on neural network and fuzzy reasoning," In ICIRA, vol. 5928, **(2009)**, pp. 1004-1012.
[38]. Y. Zhang, Y. Zhang, Z. He, and X. Tang, "Multiscale fusion of wavelet-domain hidden Markov tree through graph cut," Image Vision Comput., vol. 27, no. 9, **(2009)**, pp. 1402-1410.
[39]. P. Tracqui, "Biophysical models of tumour growth," Rep. Prog. Phys., vol. 72, no. 5, (2009), pp. 1-30.
[40]. C. Y. Liu, et al., "Study on adaptive and fuzzy weighted image fusion based on wavelet transform in trinocular vision of picking robot," J. Inf. Comput. Sci., vol. 11, no. 6, **(2014)**, pp. 1929-1937.
[41]. C. Cursiefen, et al., "VEGF-A stimulates lymphangiogenesis and hemangiogenesis in inflammatory neovascularization via macrophage recruitment," J. Clin. Invest., vol. 113, no. 7, **(2004)**, pp.1040-1050.
[42]. M. L. Si, S. Zhu, H. Wu, Z. Lu, F. Wu, and Y. Y. Mo, "miR-21-mediated tumor growth," Oncogene, vol. 26, no. 19, **(2007)**, pp. 2799-2803.

Authors

Changyu Liu, He joinedthe Communication and Computer Network Lab of Guangdong as a PhD student in 2010 at South China University of Technology, advised by Prof. Shoubin Dong. Then, he joined the School of Computer Science at Carnegie Mellon University as a Visiting Scholar in September 2012 to work with his advisor Dr. Alex Hauptmann. His research interests include machine learning and computer vision.

Bin Lu, He is currently a lecturer in the School of Computer Science at Wuyi University. He received his Ph.D. degree in 2013 from South China University of Technology. He is a reviewer of the Journal of Yangtze River Scientific Research Institute since 2010. His main research interests include complex network and machine learning.

Cong Li, received the PhD degree in Management Science and Engineering from Hefei University of Technology in 2009. He is an associate professor at the College of Computer Science, Sichuan Normal University. His research interests include E-commerce and business intelligence. He is a member of the ACM, and also is a senior member of the China Computer Federation.

